

Can massive stars form in low mass clouds?

Jamie D. Smith¹,^{*} Sarah E. Jaffa^{1,2} and Martin G. H. Krause¹

¹Centre for Astrophysics Research, Department of Physics, Astronomy and Mathematics, University of Hertfordshire, College Lane, Hatfield, Hertfordshire AL109AB, UK

²Advanced Research Computing, University College London, London WC1H 9NE, UK

Accepted 2023 September 2. Received 2023 September 1; in original form 2023 May 9

ABSTRACT

The conditions required for massive star formation are debated, particularly whether massive stars must form in conjunction with massive clusters. Some authors have advanced the view that stars of any mass (below the total cluster mass) can form in clusters of any mass with some probability (random sampling). Others pointed out that the scatter in the determinations of the most massive star mass for a given cluster mass was consistent with the measurement error, such that the mass of the most massive star was determined by the total cluster mass (optimal sampling). Here, we investigate the relation between cluster mass (M_{ecl}) and the maximum stellar mass (M_{max}) using a suite of SPH simulations. Varying cloud mass and turbulence random seed results in a range of cluster masses which we compare with their respective maximum star masses. We find that more massive clusters will have, on average, higher mass stars with this trend being steeper at lower cluster masses ($M_{\text{max}} \propto M_{\text{ecl}}^{0.31}$ for $M_{\text{ecl}} < 500 M_{\odot}$) and flattening at higher cluster masses ($M_{\text{max}} \propto M_{\text{ecl}}^{0.11}$ for $M_{\text{ecl}} > 500 M_{\odot}$). This rules out purely stochastic star formation in our simulations. Significant scatter in the maximum masses with identical initial conditions also rules out the possibility that the relation is purely deterministic (that is that a given cluster mass will result in a specific maximum stellar mass). In conclusion our simulations disagree with both random and optimal sampling of the initial mass function.

Key words: hydrodynamics – methods: numerical – stars: formation – stars: massive – galaxies: star clusters.

1 INTRODUCTION

The stellar initial mass function (IMF) is a crucial tool when studying star formation, stellar evolution, and galaxy evolution (e.g. Bastian, Covey & Meyer 2010; Guszejnov et al. 2022; Sharda & Krumholz 2022; Tanvir, Krumholz & Federrath 2022). Key features of the IMF (e.g. location of the peak, upper mass limit, and slope of the high-mass end) are all important indicators when studying the formation of stars and star clusters. There remains ongoing debate as to whether the IMF is universal – that is to say a random sample of stars taken from the IMF would be a legitimate stellar population independently of the various initial conditions (e.g. mass of parent cloud, turbulence, and local environment) that affect star formation. For example, Weidner, Kroupa & Bonnell (2010) studied a set of star clusters and their mass functions and concluded that it is unlikely that random sampling is correct for their data sample.

Studies, both observational (e.g. Weidner et al. 2010; Andrews et al. 2014) and using simulations (e.g. Bonnell, Vine & Bate 2004; Popescu & Hanson 2014), have been performed to ascertain whether there is necessarily a direct link between the mass of a cluster and the mass of its most massive star. One issue in this context is whether there is a fundamental upper limit to stellar masses (e.g. Weidner & Kroupa 2004). The most massive stars known to date are located in R136 in the Large Magellanic Cloud and are inferred to have

had initial masses $> 250 M_{\odot}$ (Brands et al. 2022). It is possible that runaway collisions further increase the star masses in massive clusters, possibly even above $1000 M_{\odot}$ (e.g. Gieles et al. 2018), but it is difficult to obtain observational evidence for such stars (Nowak, Krause & Schaerer 2022).

Weidner et al. (2010) conduct an observational study of Milky Way clusters and find that the mass of the most massive star (M_{max}) increases with cluster mass (M_{ecl}) up to $\approx 120 M_{\odot}$, with the data suggesting a power-law relation between M_{max} and M_{ecl} . Weidner, Kroupa & Pflamm-Altenburg (2013) then suggested that the scatter in the relation was purely observational uncertainties and that M_{max} was fully determined by the cluster mass. They called this an optimally sampled mass function.

Andrews et al. (2014) used the ionizing photon flux of a cluster to infer the presence of massive stars. They found clusters with fluxes that would be inconsistent with the predictions of the $M_{\text{max}}-M_{\text{ecl}}$ relation, contrary to the predictions of Weidner et al. (2013). While the findings of Andrews et al. (2014) seem conclusive, we note that their findings are based on the inferred presence of massive stars from unresolved clusters, and they note many sources of uncertainty with their data (compare also Weidner, Kroupa & Pflamm-Altenburg 2014).

Attempts have also been made to locate massive stars that do not have a nearby cluster that they could have formed in (e.g. de Wit et al. 2004; Chu & Gruendl 2008; Bestenlehner et al. 2011; Bressert et al. 2012), though the presence of bow shocks supports the theory that many of these massive field stars are runaways (e.g. de Wit et al.

* E-mail: jamie.d.smith95@gmail.com

2005; Gvaramadze & Bomans 2008). Oskinova et al. (2013) claim to have found an even more massive star with no bow shock and no obvious parent cluster candidate.

The problem was addressed theoretically by Bonnell et al. (2004). These authors simulated turbulent molecular clouds to evaluate the effect that fragmentation and competitive accretion have on the massive star formation. They find that the final mass of the most massive star is not correlated with the mass of the clump it formed from but instead is dependent on the competitive accretion that results from the continuing cluster formation. Bonnell et al. (2004) also found a correlation of the most massive star with the mass of the host cluster, measured by taking a subsample of stars around the chosen massive star in a simulation of one turbulent cloud with an initial mass of $1000 M_{\odot}$. In this work, we are expanding this study in two important ways. First, we present a suite of simulations now spanning a large range of parent cloud masses. Secondly, we investigate the statistical variations of the results by repeating each simulation multiple times with different random seeds for the generation of the initial turbulent state. We find true scatter in the $M_{\max}-M_{\text{ccl}}$ relation in clear contradiction to the deterministic expectations of optimal sampling. We also show that the dependence of our mean most-massive-star mass on cluster mass disagrees with the expectations from random sampling. In a resolution study we demonstrate that some dependence of the most massive star mass on the mass of the host cluster remains even at our highest resolution.

2 METHOD

We performed a series of smooth particle hydrodynamics (SPH) simulations of turbulent, isolated, gravitationally collapsing clouds, sweeping two different parameters. First we varied the initial mass and radius of the cloud to maintain the initial density which is the same for all simulations in this paper. This initial density is $1.62 \times 10^{-22} \text{ g cm}^{-3}$. This ensures that the initial free-fall time, $\propto 1/\sqrt{G\rho}$, is the same for all simulations. This justifies a common simulation time and comparison of the states of all simulations at the same time. Second, we increased the number of SPH particles by factors of 2 for each of the masses to see how the improvement to mass resolution affected the properties of the sink particle population.

All the simulations were performed using the SPH code GANDALF (Hubber, Rosotti & Booth 2017). We initiated isolated spherical turbulent clouds following Jaffa et al. (2022). Our simulations are isothermal at 10 K as it is a good approximation for molecular clouds at the densities that we resolve (Krumholz 2015). The virial parameter is set to 1. We simulated the system's evolution without feedback until 5 Myr has passed. We choose 5 Myr for our end time as it is long enough for a decent period of star formation but not too long that the effects of feedback would be too significant. Some simulations do not reach 5 Myr due to numerical issues such as the time-step becoming too small. Gravitational forces are computed using a KD tree (full description in Hubber et al. 2017). Sink particles are used to replace gas that surpasses a certain critical density and is not too close to an existing sink. This density criterion is resolution dependent and corresponds to resolving the Jeans mass with at least 100 SPH particles (Bate & Burkert 1997). These sink particles can accrete after they are formed but are not allowed to merge. Sink particles will accrete SPH particles that are within their accretion radius and are gravitationally bound to the sink. All this follows the original setup of Bonnell et al. (2004) closely.

Various forms of feedback have been implemented in recent simulations of star formation. They generally damp the growth of stars, with some forms being particularly effective at inhibiting

growth at higher star masses (Bastian et al. 2010; Guszejnov et al. 2022; Sharda & Krumholz 2022; Tanvir et al. 2022). In this paper, we neglect any form of feedback as it would only inhibit the formation of massive stars. Our most massive stars already fall short of observed star masses at the high-mass end at the chosen end time of our simulations. Additionally, any effect of feedback would have to affect high- or low-mass clusters differently to significantly change our results.

For the mass variation, we simulate clouds spanning the mass range 1000 to $40\,000 M_{\odot}$. The radii of the clouds are varied to maintain constant initial density across the different masses. We take the simulation with a mass of $10\,000 M_{\odot}$ a radius of 10 pc and 100 000 SPH particles as fiducial with the others adjusted accordingly. We control the mass resolution rather than the number of SPH particles so that we can directly compare without considering the affect that mass resolution has on the sink particle masses. See full details in Table 1.

For the resolution variation, we repeatedly double the number of SPH particles until the simulations become prohibitively computationally expensive, a resolution indicator of 1 means that there are 10 particles per solar mass. The sink particle formation criteria are also adjusted adhering to SPH resolution, where we adjust the sink particle critical density such that a sink particle will form from at least 100 SPH particles (Bate & Burkert 1997). Therefore at 1 resolution the minimum mass of a sink particle is $10 M_{\odot}$. This set of simulations also serves to bring clarity to the massive star versus small association ambiguity found in our more massive simulations (e.g. the $40\,000 M_{\odot}$ res = 1 simulation) described above by allowing a small association to be resolved into individual sink particles.

For all of the simulation specifications above, we perform 10 simulations varying the random seed used to create the turbulent field. We do this to obtain a statistically significant result by reducing the errors inherent in a simulation of a chaotic system (Jaffa et al. 2022).

We investigate the IMF of the sink particles in order to analyse key properties of the sink population. We look at the maximum mass of a sink particle achieved in order to study how the total cloud mass affects the maximum sink particle mass. The minimum mass found in the sink population will be limited by the mass resolution (Bate & Burkert 1997). Therefore the minimum mass possible will scale inversely with the number of SPH particles. The presence of a power-law slope in the high-mass region of the IMF serves as a sanity check that we have a realistic distribution of stellar masses.

We investigate the masses of the most massive sink particles for each simulation as well as the mean and standard deviation. This shows us the maximum mass for each simulation, the spread for a given mass, and whether the maximum masses had converged. We use the standard deviations to estimate how many simulations at a given mass we would need to perform to be likely to form a star as massive as we find in our $10\,000 M_{\odot}$ at the same respective resolution. We choose $10\,000 M_{\odot}$ for the comparison as the higher masses often do not run for the full duration due to numerical problems and therefore their stellar and cluster masses are understated. We also look at how the maximum mass changes with mass resolution by plotting the relation between the average cluster mass and average maximum stellar mass at multiple resolutions. This allows us to see the effect that mass resolution has on the star formation and demonstrates the importance of comparing results at the same mass resolution.

To examine the possibility that our clusters could be considered to be multiple smaller clusters, we use a friend-finding algorithm (Davis et al. 1985). This algorithm separates our clusters into groups

Table 1. Table contains simulation specifications and results averaged according to simulation mass and resolution. $\alpha_{<500}$ and $\alpha_{>500}$ are power-law slopes corresponding to fits to most-massive star masses over clusters masses below and above $500 M_{\odot}$, respectively. ‘Required Sims’ is the number of simulations we would need to run before we would expect to find a star with the average maximum mass formed in the $10\,000 M_{\odot}$ simulations at the same resolution.

Sim mass (M_{\odot})	Sim res	$\alpha_{<500}$	$\alpha_{>500}$	Avg time (Myr)	Avg M_{\max} (M_{\odot})	M_{\max} (M_{\odot})	Sigma (M_{\odot})	Avg M_{ecl} (M_{\odot})	Required sims
1000	1.0	0.651	0.173	5.00	27.600	69.1	24.481	37.160	36 107 909
1500	1.0	0.651	0.173	5.00	55.080	114.6	32.290	98.780	1287
2500	1.0	0.651	0.173	5.00	94.140	168.2	34.915	249.130	22
5000	1.0	0.651	0.173	5.00	143.000	232.9	42.604	694.650	2
10000	1.0	0.651	0.173	5.00	163.600	242.2	40.025	1753.990	1
20000	1.0	0.651	0.173	5.00	203.889	253.0	26.702	4129.922	1
40000	1.0	0.651	0.173	5.00	223.300	346.4	58.606	9843.800	1
1000	2.0	0.431	0.106	5.00	31.510	70.2	23.548	47.650	384 116
1500	2.0	0.431	0.106	5.00	55.000	98.8	20.735	110.100	38 214
2500	2.0	0.431	0.106	5.00	91.540	148.0	29.371	260.130	12
5000	2.0	0.431	0.106	5.00	114.520	168.2	32.906	704.370	3
10 000	2.0	0.431	0.106	5.00	142.180	195.8	31.139	1758.270	1
20 000	2.0	0.431	0.106	5.00	146.240	186.3	26.914	4197.380	1
40 000	2.0	0.431	0.106	4.93	164.990	289.4	47.926	9041.080	1
1000	4.0	0.377	0.064	5.00	29.730	50.7	14.853	53.310	262 396
1500	4.0	0.377	0.064	5.00	48.790	89.2	19.651	112.310	86
2500	4.0	0.377	0.064	5.00	62.680	112.3	27.166	266.700	6
5000	4.0	0.377	0.064	5.00	89.310	138.4	25.435	701.880	2
10 000	4.0	0.377	0.064	5.00	98.370	127.4	15.182	1750.450	1
20 000	4.0	0.377	0.064	5.00	102.400	130.5	14.611	4127.160	1
40 000	4.0	0.377	0.064	4.90	117.530	139.6	16.606	8477.050	1
1000	8.0	0.367	0.133	5.00	24.930	49.9	11.731	56.150	16 002
1500	8.0	0.367	0.133	5.00	35.390	59.9	14.758	119.330	75
2500	8.0	0.367	0.133	5.00	46.510	92.0	19.445	270.970	6
5000	8.0	0.367	0.133	5.00	61.820	108.2	20.857	698.420	2
10 000	8.0	0.367	0.133	4.98	71.890	111.7	19.085	1659.890	1
20 000	8.0	0.367	0.133	4.82	72.540	92.7	10.708	3401.650	1
40 000	8.0	0.367	0.133	4.58	79.510	99.4	13.083	6520.150	1
1000	16.0	0.437	0.209	5.00	18.640	36.1	9.401	57.820	1990
1500	16.0	0.437	0.209	5.00	23.830	48.6	11.145	120.450	74
2500	16.0	0.437	0.209	5.00	36.900	61.8	13.904	263.140	4
5000	16.0	0.437	0.209	5.00	43.270	51.4	7.574	683.910	4
10 000	16.0	0.437	0.209	4.91	51.350	70.1	12.500	1585.600	1
20 000	16.0	0.437	0.209	4.30	47.920	60.9	11.209	2299.410	1
40 000	16.0	0.437	0.209	3.92	48.970	85.9	13.800	3665.310	1
1000	32.0	0.313	0.113	5.00	12.840	24.6	6.926	57.650	73
1500	32.0	0.313	0.113	5.00	18.460	39.5	7.881	120.930	7
2500	32.0	0.313	0.113	4.90	20.470	27.9	4.468	229.040	29
5000	32.0	0.313	0.113	4.81	25.170	31.2	4.508	514.930	4
10 000	32.0	0.313	0.113	4.66	29.880	41.5	7.448	1152.830	1
20 000	32.0	0.313	0.113	4.26	30.800	41.1	5.641	2156.540	1
40 000	32.0	0.313	0.113	3.48	28.550	37.3	6.535	2274.490	1

according to a ‘linking length’, a group is then made of any sink particles that can be joined by no more than this length.

3 RESULTS AND ANALYSIS

At our highest resolution, the mass of the most massive stars in our simulations correlates with the mass of the cluster formed (Fig. 1). This behaviour is expected from both random sampling and optimal sampling, as can be seen in Fig. 1: The red-dashed line shows the mean maximum star mass expected for random sampling, and the solid black line shows the exact value for the most massive star for a given cluster mass for optimal sampling. While the two lines are similar, we expect the most massive star masses to be scattered around the lines for random sampling, but exactly on the line for optimal sampling if the respective sampling method was a faithful description of our simulations. Our simulations clearly show a scatter

of most massive star masses for any given cluster mass, which is in general agreement with the random sampling concept. It is possible that our clusters could be considered to be comprised of multiple smaller clusters. To address this we use a friend-finding algorithm to group the sink particles according to a ‘linking length’. We find that the clusters have no preferred scale with the grouping changing smoothly with the linking length. This makes sense for a cluster formed from a cloud with decaying turbulence.

Fig. 1 (bottom) shows the results for an example linking length of 1 pc changes are subtle. Overall, the result is very similar to taking all stars in a given simulation as a cluster (Fig. 1, top). For full-simulation clusters and below a cluster mass M_{ecl} of $500 M_{\odot}$, we find for the mass of the most massive star, $M_{\max} \propto M_{\text{ecl}}^{\alpha}$ with $\alpha = 0.31 \pm 0.05$. For $M_{\text{ecl}} > 500 M_{\odot}$ α flattens to 0.07 ± 0.08 . The values for α are consistent within uncertainties for the clusters defined via the group-finding algorithm. The scatter around these lines is similar

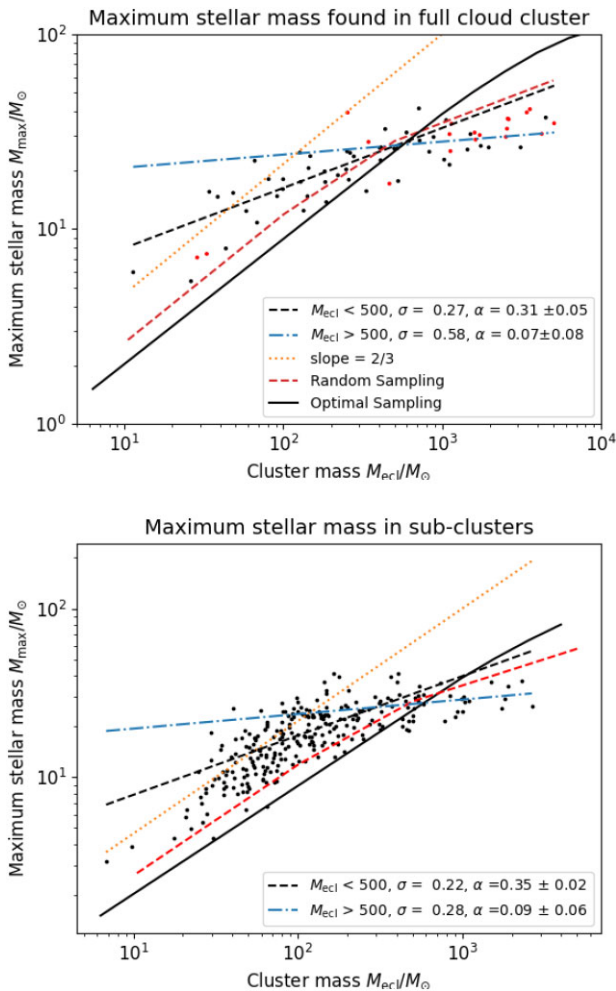


Figure 1. *Top:* Maximum star mass against total stellar mass in all of the highest resolution (32 resolution) simulations. Random sampling plotted as red-dashed line, created using mass constrained random sampling from a Kroupa IMF up to $150 M_{\odot}$. Optimal sampling plotted as a solid black line from Weidner et al. (2010). Dotted line shows an exponent of $2/3$ (Bonnell et al. 2004). Simulations that did not reach the full runtime are plotted as red dots (at least 90 percent of the nominal runtime), black dots represent completed simulations. Black dashed and blue dotted-dashed lines show power-law fit lines to our data below and above $M_{\text{ecl}} = 500 M_{\odot}$, respectively. In the legend, we give the respective power-law index (α) with uncertainties (one standard deviation) from the fit as well as a measure of the scatter of the data points around the fit line (σ , also one standard deviation). *Bottom:* The same plot as the top panel but each cluster is split into groups using a friend-finding algorithm. Each group is then treated as its own cluster.

below $500 M_{\odot}$. Above this limit, the scatter is somewhat reduced for the clusters defined by the group-finding algorithm.

Improving the mass resolution of the simulations alters the IMF (Fig. 2) in a number of ways. First, we can see that the low-mass end shifts to lower masses with improved resolution as expected, we also see a shift to lower masses in the rest of the IMF following the low-mass end, finally we see that the high-mass end peaks at lower masses as we increase the resolution.

These results might suggest that there is a critical cloud mass required to form massive stars. In our simulations, this critical mass is resolution dependent. In our low-resolution simulations, we require a cloud mass of $5000 M_{\odot}$ to form a sink particle above $100 M_{\odot}$. At our highest resolution, we find a critical cloud mass of $10000 M_{\odot}$

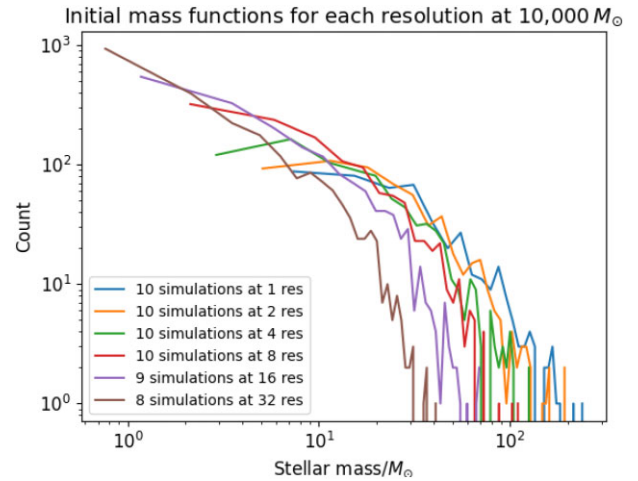


Figure 2. The initial mass function of the $10000 M_{\odot}$ simulations for the range of resolutions as labelled.

required to produce a sink mass of $40 M_{\odot}$ (Fig 3). In Table 1, we show the level of outlier required for each simulation setup to produce the average maximum mass found in the $10000 M_{\odot}$ simulation of the same resolution. We see that, at the highest resolution, for a $1000 M_{\odot}$ simulation a 2.46σ outlier is required to form the average mass found in our $10000 M_{\odot}$ simulations. This corresponds to needing 72 simulations of $1000 M_{\odot}$ to form the $10000 M_{\odot}$ average. Since the mass ratio between the two setups is only a factor of 10, this means that stars towards the upper mass end of the $10000 M_{\odot}$ cloud form much less frequently in our $1000 M_{\odot}$ clouds than what would be expected from random sampling from the IMF from our 10000 solar mass clouds.

This decrease in the maximum mass is better seen by looking at the distribution of maximum masses directly (Fig. 3). This clearly shows the masses decreasing with each increase in resolution, this is expected as the better resolution allows us to resolve the larger dense regions into multiple sink particles rather than fewer large sink particles.

The higher mass ($40000 M_{\odot}$) resolution study shows the same trends (Fig. 3). This also allows us to see that the very high mass ($>200 M_{\odot}$) sink particles seen in Fig. 3 are most likely representing an unresolved group. We see that the maximum stellar masses drop as we increase resolution, as the potential for sink particles to represent many individual stars is reduced, so is the variation on the sink mass reduced to the variation of the mass of an individual star. Resolution is further examined in the Appendices.

From the mass evolution of the most massive star over time (Fig. 4) we see that the final most massive star has been the most massive throughout the simulation time in approximately half of the simulations. In the majority of cases, the star appears to still be growing, however, this growth is significantly reduced in the lower mass simulations except for a few cases. In the cases where we see a late forming star become the most massive, it is often the case that the previous most massive is only growing slowly due to it having exhausted its local reservoir. The resolution dependence of the maximum stellar mass is not sufficiently explained by lower formation mass (due to aforementioned resolution criteria), instead it is due to complex structure in the gas leading to erratic bursts of higher accretion.

Fig. 5 shows the mass evolution of the most massive star with the cluster mass. In the lower mass simulations, we see that the most

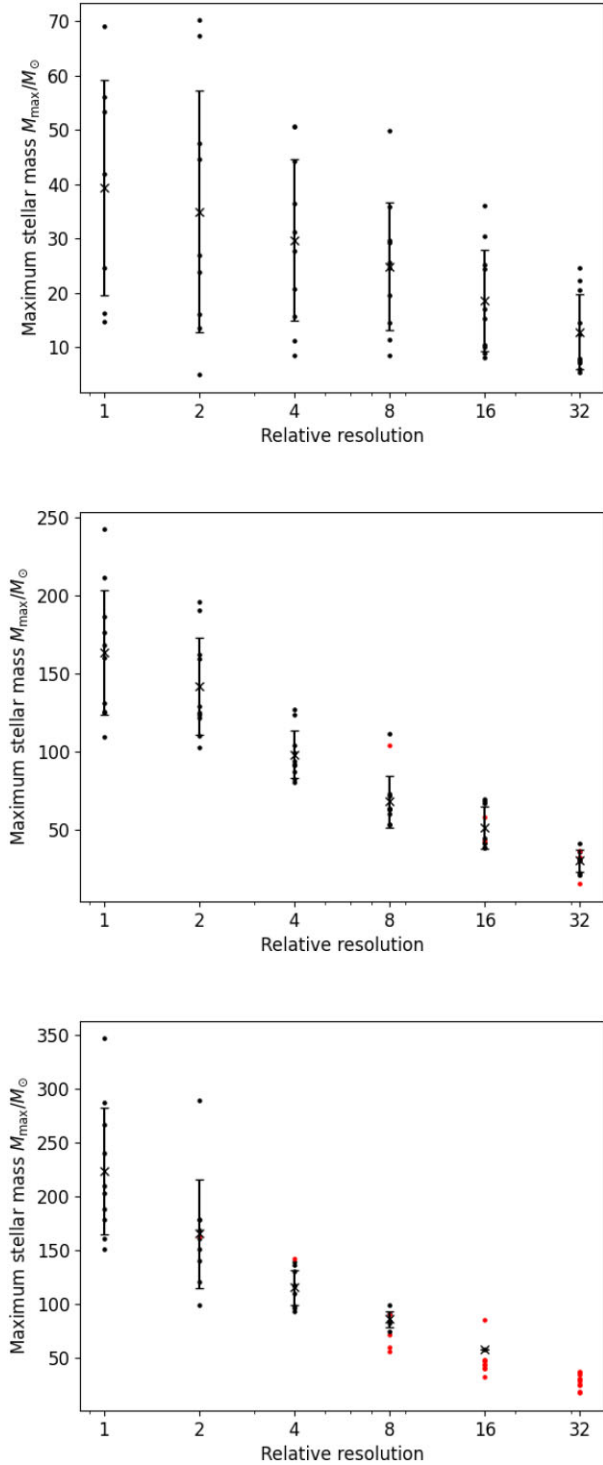


Figure 3. Distribution of maximum sink particle mass as we increase the mass resolution for the *Top*: $1000 M_{\odot}$, *Middle*: $10\,000 M_{\odot}$, and *Bottom*: $40\,000 M_{\odot}$ simulations. The maximum sink mass decreases with resolution as expected, it increases with increased cloud mass between the $1000 M_{\odot}$ and the $10\,000 M_{\odot}$ plots. There is less difference between the $10\,000 M_{\odot}$ and the $40\,000 M_{\odot}$. The red dots indicate simulations that did not run to completion, these are removed from calculations of the error bars.

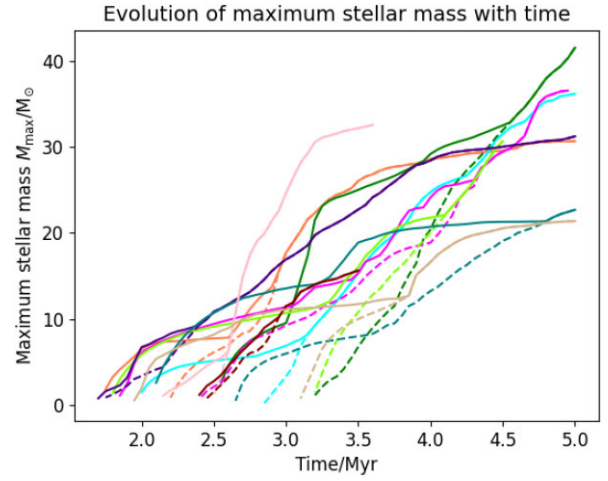


Figure 4. Mass evolution of the final most massive star (dashed line) as well as the highest mass at each time (solid line) for each random seed with 32 resolution and initial cloud mass $10\,000 M_{\odot}$.

massive stars are found in the most massive clusters. This is less the case in the higher mass simulations where the majority of the clusters reach $>500 M_{\odot}$. The dominant impression of leveling off in these plots means that while the most massive star quickly exhausts its immediate environment, other regions of the cluster keep growing steadily at late times. There is an interesting case at a cloud mass of $1500 M_{\odot}$, where we find one simulation where the most massive star keeps growing strongly and in proportion with the rest of the cluster, until it reaches $40 M_{\odot}$ at a cluster mass of only $250 M_{\odot}$. This illustrates that occasionally, very high mass stars can form in relatively low-mass clusters in our simulations (Fig. 6).

The behaviour seen with mass evolution against cluster mass (Fig. 5) is split at $M_{\text{ecl}} \sim 500 M_{\odot}$. Below this we see a consistent positive correlation between cluster mass and star mass, above this the maximum star mass depends more on the cloud mass, this becomes more prominent if we factor in the shorter average runtime of the higher mass simulations. While resolution does affect the sink masses significantly, due to the minimum possible mass and ability to resolve large sinks into multiple smaller sinks, this affect is fairly consistent across the different masses (Fig. 3 and Appendix A Fig. A1).

4 DISCUSSION

The suite of simulations presented here consistently displays certain trends found when varying both the cloud mass and the mass resolution. We see that an increase in the cloud mass invariably leads to higher mass sink particles being formed, this trend is subtle at higher cloud masses but is very obvious up to the intermediate cloud masses ($\sim 2000 M_{\odot}$). While the more extreme of these massive sink particles can be explained as unresolved groups (as indicated by their absence at higher resolution) this trend is still apparent when comparing the highest mass resolution simulations (Fig. 3). However, very rarely, we also find very high mass stars in comparatively low-mass clusters (see $1500 M_{\odot}$ in Fig. 5).

This would suggest that the very high mass stars found in apparent isolation (e.g. Bestenlehner et al. 2011; Bressert et al. 2012; Oskinova et al. 2013) either did not form in isolation or they formed under extreme circumstances not included in our simulations.

We see in Fig. 1 that the maximum star mass increases with cluster mass a trend that appears, in principle, consistent with the findings presented by Weidner et al. (2013; see their fig. 1). We also see

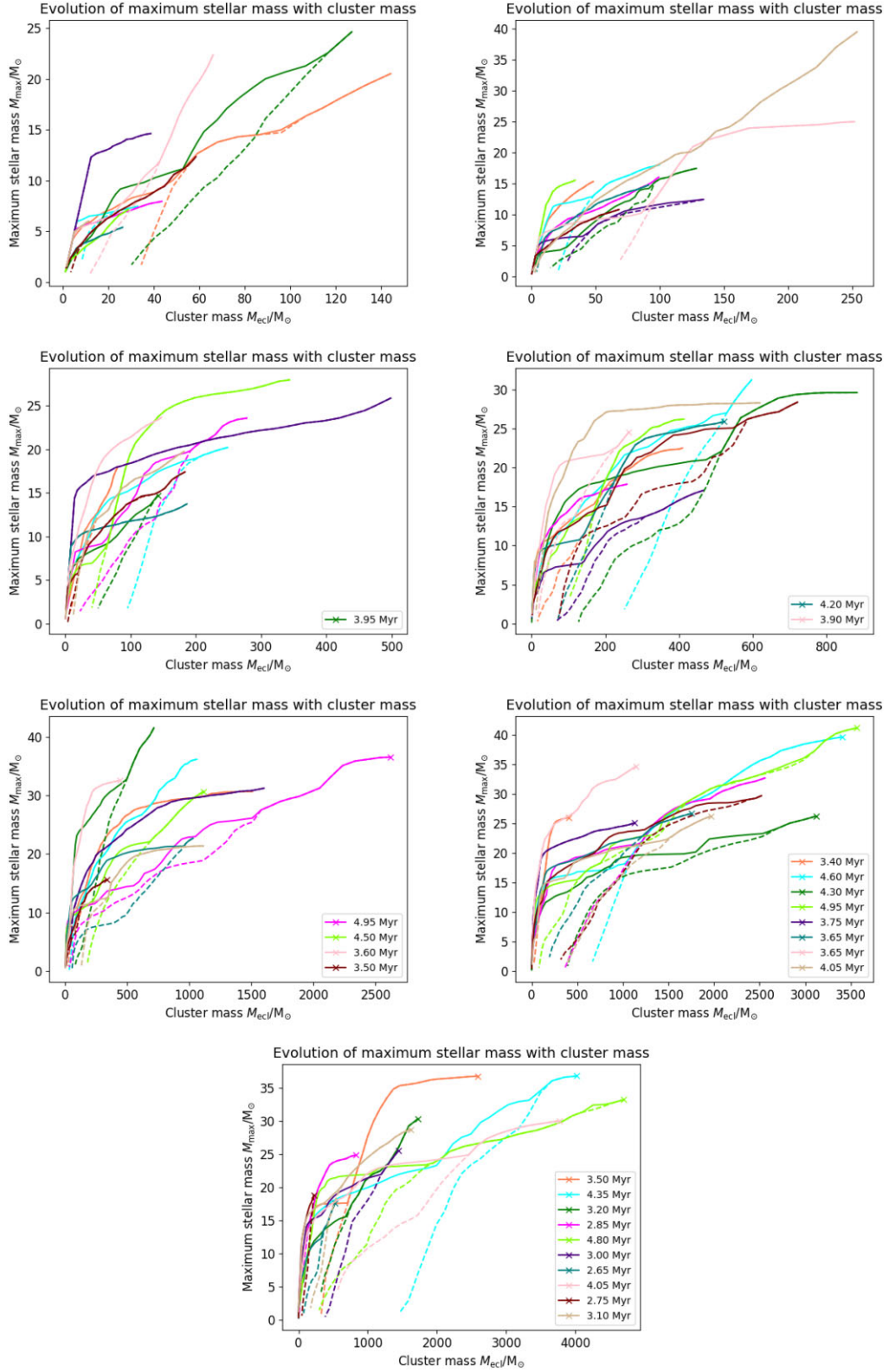


Figure 5. The evolution of the mass of the most massive star against the cluster mass. Solid line represents the most massive star at that time while the dashed line tracks the star that will end up as the most massive. Resolution and simulation mass labelled. A ‘x’ indicates that that individual simulation did not reach 5 Myr, the end times are labelled in these cases.

Downloaded from https://academic.oup.com/mnras/article/525/4/6182/7263272 by University of Hertfordshire user on 15 November 2023

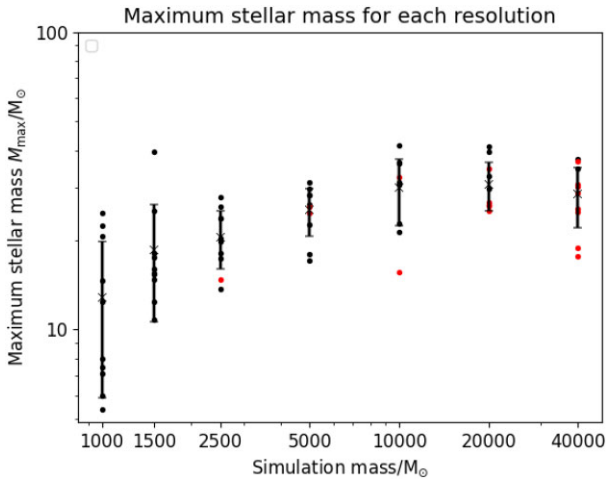


Figure 6. Distribution of maximum star masses found in each of the simulations, we examine at their maximum mass resolution. Red dots indicate a simulation that did not run for at least 4.5 Myr.

significant scatter in the maximum mass for a given cloud mass, this spread decreases with increased cloud mass. This suggests that the spread Weidner et al. (2013) find may be less due to observational uncertainty and more due to actual variation than they suggest. The findings shown in our Fig. 3 at first appear inconsistent with the idea of purely stochastic star formation. At all resolutions we see higher mass stars in higher mass clusters. There is, however, a scatter involved, and had we carried out even more simulations, we might have found even higher most-massive-star values. To quantify this we compared each simulation (cloud) mass to the $10\,000\,M_{\odot}$ simulations at the same respective resolution. We calculate how many low-mass clusters on average are required to form a star of the same mass. We see that for low mass clusters to form a star with the average maximum mass of a high-mass cluster (e.g. $10\,000\,M_{\odot}$) would also form more cluster mass than is required on average for the $10\,000\,M_{\odot}$ simulation, for example 72 simulations at $1000\,M_{\odot}$ would form over $4000\,M_{\odot}$ of cluster mass (almost 4 times more than the single $10\,000\,M_{\odot}$ simulation). This is in clear disagreement with the expectations of purely random sampling where the same total cluster mass should produce the same massive stars on average. We see the largest change in maximum mass seen between cloud masses 1000 and $5000\,M_{\odot}$ after which the change is slighter as the mass increases. The maximum mass averaged over each repeat simulation also increases up to $10\,000\,M_{\odot}$. However, it remains fairly consistent after that point. From our look at potential sub-clusters, we find that in both cases the most-massive-star mass against cluster mass becomes shallower at $500\,M_{\odot}$ but the power-law slopes are consistent within the uncertainties. The scatter decreases in both the high-mass and low-mass groups, though the change is greater at the high-mass end. This makes sense as the maximum mass will remain the same while the sub-cluster mass will be lower than the combined cluster.

We observe that our most-massive-star mass with cluster-mass differs in detail to both the expectations of random sampling and optimal sampling (compare Fig. 1). At high cluster masses, our most-massive-star masses are below the expectations, whereas at low cluster masses we find higher star masses than expected. Yet, our quantitative analysis in Table 1 shows that in order for all our clusters to be randomly sampled from the same mass function we would need to see even higher mass stars in our low mass clusters. This apparent contradiction demonstrates that our clusters are not

randomly sampled from the Kroupa IMF. Looking at Fig. 2, we see that as we increase resolution our mass functions get steeper, approaching the Kroupa IMF. At the same time, at higher resolution we need fewer low-mass clusters to get a most-massive-star as massive in a high cluster-mass simulation, in better agreement with random sampling of a uniform IMF. This gives reason for hope that in the future even higher resolution simulations will agree with observations.

Fig. 4 shows the mass evolution against time for the $10\,000\,M_{\odot}$ mass clouds at our highest resolution. We see that in all of the simulations the most massive star continues to grow, though the rate of growth varies with random seed. This is likely due to variation in the rate of accretion on to the system from the surrounding cloud. After their initial burst of growth the star growth slows, either almost flattening out or becoming ‘clumpy’. The stars that flatten out are often overtaken by late forming stars with more rapid growth. This behaviour is possibly due to gas supply with growth slowing when the stars birth clump is depleted and further growth relying on gas being funnelled into the system. This could either be slow and steady or clumpy resulting in the erratic rate of growth we see in some of the stars.

To look at the effects that the physics missing from our simulations may have had, we compare our results to those from Guszejnov et al. (2022). They find that adding feedback to their simulations decreases the maximum mass found. Their resulting most massive stars in their ‘M2e4_C_M_J’ simulations are of similar mass to our higher mass simulations. Grudić et al. (2023) perform a similar study to ours simulating many lower mass clusters with feedback. They too find that a single larger cluster will produce more massive stars than many lower mass clouds.

5 SUMMARY AND CONCLUSIONS

In this paper, we analysed the statistical properties of the massive-star populations that form for molecular clouds with a range of different masses. The goal was to see if there was a significant difference for star formation in low-mass star clusters and high-mass star clusters. We consider two extremes: first that star formation is purely stochastic and a given combined stellar mass will be comprised of stars of statistically the same masses independently of whether they were in a single very massive cluster or many low mass clusters (random sampling). Secondly, that star formation is completely deterministic and that for a given cluster mass there is a set maximum stellar mass (*Optimal Sampling*; Kroupa et al. 2013).

Our simulations do not entirely agree with either of the above options. We see significant scatter in the maximum star mass produced from the same initial conditions. This rules out deterministic star formation, though we note that various forms of feedback missing from our simulations could potentially inhibit accretion once a star reaches a certain mass and thus reduce the scatter. We also find a significant trend, most noticeable at lower masses, between cluster mass and maximum star mass. We also find a critical mass requirement to form stars above a certain mass ($40\,M_{\odot}$ stars are not found below a cluster mass of $500\,M_{\odot}$ in our highest resolution simulations). These combined show that in our simulations star formation cannot be purely stochastic.

From the calculated standard deviations of the stellar masses for each cloud mass and simulation resolution we also see that the probability of a low mass cloud forming a star as massive as are often formed from high mass clouds is sufficiently low so that we would need to form much more cluster mass before we would expect to see a star of similar mass to the higher mass simulation

(4 times the cluster mass from the simulations with cloud masses of 1000 versus 10 000 M_{\odot} , respectively, compare above). Therefore, our low-mass clusters are not randomly sampled from our high-mass clusters' distributions. This further disagrees with purely stochastic star formation which predicts the massive star population to be consistent with total cluster mass. Compared to both random and optimal sampling based on observed initial mass functions, our low-mass clusters still form too many massive stars. On the other hand, our high-mass clusters do not reach observed massive star masses. We note that the required number of low-mass-cluster simulations to yield a most-massive star as massive as in a higher mass simulation decreases with increased resolution. It is thus possible that at very high resolution we may see agreement with random sampling.

We see from the evolution for maximum stellar mass with cluster mass (Fig. 5) that the paths the most massive stars take varies significantly. While sometimes an early forming star will steadily accrete and end up as the most massive star in the cluster, it is also common for the early forming star's growth to slow significantly and for a late forming star to overtake with more rapid accretion. This demonstrates that the star that eventually becomes the most massive star is not 'linearly' pre-determined by the initial conditions, but emerges dynamically by the non-linear behaviour of the system.

ACKNOWLEDGEMENTS

SJ acknowledges support from the STFC grant ST/R00905/1. JDS acknowledges a studentship from the Science and Technology Facilities Council (STFC) (ST/T506126/1). We thank the reviewer for their helpful suggestions and constructive criticism.

DATA AVAILABILITY

Data and full running instructions available on request: j.smith49@herts.ac.uk

REFERENCES

Andrews J. E. et al., 2014, *ApJ*, 793, 4
 Bastian N., Covey K. R., Meyer M. R., 2010, *ARA&A*, 48, 339
 Bate M. R., Burkert A., 1997, *MNRAS*, 288, 1060
 Bestenlehner J. M. et al., 2011, *A&A*, 530, L14
 Bonnell I. A., Vine S. G., Bate M. R., 2004, *MNRAS*, 349, 735
 Brands S. A. et al., 2022, *A&A*, 663, A36
 Bressert E. et al., 2012, *A&A*, 542, A49
 Chu Y. H., Gruendl R. A., 2008, in Beuther H., Linz H., Henning T., eds, *Massive Star Formation: Observations Confront Theory*. Astron. Soc. Pac., San Francisco, p. 415
 Davis M., Efstathiou G., Frenk C. S., White S. D. M., 1985, *ApJ*, 292, 371
 de Wit W. J., Testi L., Palla F., Vanzi L., Zinnecker H., 2004, *A&A*, 425, 937
 de Wit W. J., Testi L., Palla F., Zinnecker H., 2005, *A&A*, 437, 247
 Gieles M. et al., 2018, *MNRAS*, 478, 2461
 Grudić M. Y., Offner S. S. R., Guszejnov D., Faucher-Giguère C.-A., Hopkins P. F., 2023, , preprint(arXiv:2307.00052)
 Guszejnov D., Grudić M. Y., Offner S. S. R., Faucher-Giguère C.-A., Hopkins P. F., Rosen A. L., 2022, *MNRAS*, 515, 4929
 Gvaramadze V. V., Bomans D. J., 2008, *A&A*, 490, 1071
 Hubber D. A., Rosotti G. P., Booth R. A., 2017, *MNRAS*, 473, 1603

Jaffa S. E., Dale J., Krause M., Clarke S. D., 2022, *MNRAS*, 511, 2702
 Kroupa P., Weidner C., Pflamm-Altenburg J., Thies I., Dabringhausen J., Marks M., Maschberger T., 2013, in Oswald T. D., Gilmore G., eds., *Dordrecht, Planets, Stars and Stellar Systems. Volume 5: Galactic Structure and Stellar Populations, Vol. 5*. p. 115
 Krumholz M. R., 2015, Notes on star formation, , preprint(arXiv:1511.03457)
 Nowak K., Krause M. G. H., Schaerer D., 2022, *MNRAS*, 516, 5507
 Oskinova L. M., Steinke M., Hamann W. R., Sander A., Todt H., Liermann A., 2013, *MNRAS*, 436, 3357
 Popescu B., Hanson M. M., 2014, *ApJ*, 780, 27
 Sharda P., Krumholz M. R., 2022, *MNRAS*, 509, 1959
 Tanvir T. S., Krumholz M. R., Federrath C., 2022, 516, 13, *MNRAS*
 Weidner C., Kroupa P., 2004, *MNRAS*, 348, 187
 Weidner C., Kroupa P., Bonnell I. A. D., 2010, *MNRAS*, 401, 275
 Weidner C., Kroupa P., Pflamm-Altenburg J., 2013, *MNRAS*, 434, 84
 Weidner C., Kroupa P., Pflamm-Altenburg J., 2014, *MNRAS*, 441, 3348

APPENDIX A: RESOLUTION STUDY

We show mean most massive star masses with 1σ variation between different realizations of the same simulation mass over the total mass in the simulations in Fig. A1. We do this to easily display the differences both mass and resolution have on the maximum mass. We see that maximum mass is well correlated with simulation mass and anticorrelated with simulation resolution.

We plot the maximum sink particle mass over cluster mass for every simulation (all that formed sink particles) and these are shown in Fig. A2. We see again that higher resolution consistently reduces maximum stellar mass and that higher simulation cloud mass results in higher maximum stellar mass, the cloud mass dependence is stronger at lower resolutions but is still present at our highest resolution with maximum masses increasing more steeply until about 600 M_{\odot} where we see the trend flatten.

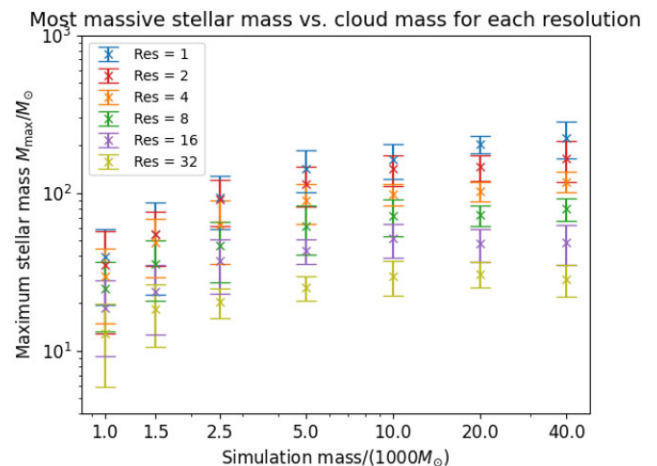


Figure A1. Average maximum mass for each simulation cloud mass at each resolution. One standard deviation plotted as error bars, see legend for correspondence between colours and resolution. The maximum star mass decreases monotonically with increasing resolution for all simulated clouds. For all resolutions, the maximum star mass increases up to 5000 M_{sun} , and then stays roughly constant with simulation mass.

Maximum stellar mass against cluster mass for each resolution

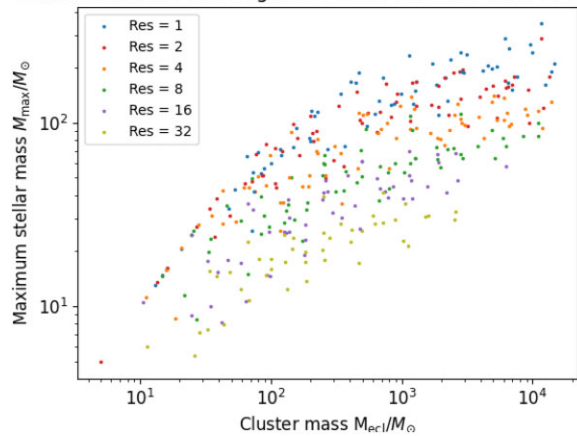


Figure A2. Maximum stellar mass against cluster mass for all simulations, with the resolutions indicated by colour as labelled. A stellar mass limit is reached for a given cluster mass which decreases with increasing resolution.

This paper has been typeset from a $\text{\TeX}/\text{\LaTeX}$ file prepared by the author.